

# Unsteady 3D MHD Carreau and Casson Fluids over a Stretching Sheet with Non-Uniform Heat Source/Sink

Mamatha S. U<sup>1\*</sup> C.S.K.Raju<sup>1\*</sup> G. Madhavi<sup>1</sup> Mahesha<sup>3</sup>

1.Department of Computer Science, Garden City University, Bangalore-560049, India

2.Department of Mathematics, UBDT College of Engineering, Dhavangere, India

## Abstract

In this study, we analyzed the effects of nonlinear thermal radiation and non-uniform heat source/sink on an unsteady three-dimensional flow of Carreau and Casson fluid past a stretching surface. The transformed governing equations are solved numerically using Runge-Kutta based shooting technique. We obtained better accuracy of the present results by comparing with the already published literature. The influence of dimensionless parameters on velocity and temperature profiles along with the friction factors, local Nusselt and Sherwood numbers are discussed with the help of graphs and tables. We presented dual nature solutions for the flow over a Carreau and Casson fluid cases. It is also found that the non-uniform heat source or sink is control the thermal boundary layer for both the Casson and Carreau fluid cases.

**Keywords:** MHD, unsteady, nonlinear thermal radiation, Carreau fluid, Casson fluid, 3D.

## Introduction

Convection boundary layer flow over a kinetic stretching sheet has relevance in many engineering processes such as drawing of plastic films, tinning and annealing of copper wires and electrolyte paper production etc. Due to these applications Sakiadis [1] started the flow past a stretching sheet. After, the many researchers are studied under various interesting aspects in [2]-[6]. On the other hand flow past a non-Newtonian fluid flows are encountered in several large-scale industrial applications including blood flows in micro-circulatory system, food and polymer processing, magma and ice flows. Casson fluid is also a non-Newtonian fluid, which shear thinning liquid and exhibits the yield shear stresses. If a yield stress is greater than the shear stress it acts as a solid, whereas if a yield stress is lesser than shear stress is applied, the fluid would be starts to move. For example honey, tomato sauce, fruit juices and human blood. It has various applications in fibrinogen, cancer homeo-therapy, protein and red blood cells form a chain type structure. Due to flow diversity in the environment a single mathematical model is not overcomes all the rheological fluid properties associated with non-Newtonian fluids. Thus various constitutive equations for such fluids are available in already existing literature [7-12]. Additionally, the Power-law Carreau fluid is also one of the non-Newtonian fluid model. Carreau fluid model is valid for viscous, high and low shear rates. Because of this it has benefitted in many technological and manufacturing flows. By taking this into inspiration the authors [13-14] studied the non-Newtonian fluid with two geometries (asymmetric channel and cone).

Magnetohydrodynamic (MHD) is the mechanical property of fluids, which describes the motion of highly conducting fluid with existing of magnetic field. The conducting fluids are generates an electric current in the fluid flow and this force can be boost up the mechanical properties of fluid flow. Due to these applications the more researchers are concentrating on this field. The motivated by the above application the more investigated are done in this area. Which are given in ref. [15-20]. Recently, heat transfer in the flow over a stretching sheet with non-uniform heat source or sink effect have major role in metallurgy and chemical engineering industries, such as polymer production and food processing. Moreover, coupled heat and mass transfer problems in the presence of homogeneous-heterogeneous reaction are of importance in many processes, and have therefore it is a considerable amount of attention in recent days. Therefore some of the possible applications can be found in processes such as drying, damage of crops due to freezing, distribution of temperature and moisture over agricultural fields and groves of fruit trees, evaporation at the surface of a water body and energy transfer in a wet cooling tower. The three dimensional flow through stretching has great attention due to its importance in various fields like MHD accelerators, Generators, pumps and flow meters, design of cooling systems these are given by [21-28].

Motivation of above studies, In this study we proposed a mathematical model for the effects of nonlinear thermal radiation and non-uniform heat source/sink on an unsteady three-dimensional flow of Carreau and Casson fluids past a stretching surface. The transformed governing equations are solved numerically using Runge-Kutta based shooting technique. We obtained better accuracy of the present results by comparing with the already published literature. The influence of dimensionless parameters on velocity and temperature profiles along with the friction factors and local Nusselt number are discussed with help of the graphs and tables.

## Formulation of the problem

In this article we present a mathematical model for 3D an unsteady convection flow of a Carreau fluid flow in

the presence of nonlinear thermal radiation and non-uniform heat source/sink. The flow is restricted to  $z$  – direction. In this study we skip the induced magnetic field. The flow is due to stretching surface. The extra stress tensor for the proposed Carreau fluid is given by

$$\bar{\tau}_{ij} = \eta_0 \left[ 1 + \frac{(n-1)}{2} \Gamma^2 (\bar{\dot{\gamma}})^2 \right] \bar{\dot{\gamma}}_{ij}, \quad (1)$$

$$\text{where } \bar{\dot{\gamma}} = \sqrt{\frac{1}{2} \sum_i \sum_j \bar{\dot{\gamma}}_{ij} \bar{\dot{\gamma}}_{ji}} = \sqrt{\frac{1}{2} \Pi}, \quad (2)$$

in which  $\bar{\tau}_{ij}$  is the stress tensor,  $\eta_0$  is the zero viscous shear rate,  $n$  is the power-law index,  $\Gamma$  is the time constant,  $\Pi$  is the invariant second strain tensor, according to our assumption the Carreau model is given by:

**Flow Analysis:**

$$\frac{\partial u}{\partial x} + \frac{\partial v}{\partial y} + \frac{\partial w}{\partial z} = 0, \quad (3)$$

$$\left( \frac{\partial u}{\partial t} + u \frac{\partial u}{\partial x} + v \frac{\partial u}{\partial y} + w \frac{\partial u}{\partial z} \right) = \nu \left( \left( 1 + \frac{1}{\beta} \right) \frac{\partial^2 u}{\partial z^2} + \frac{3(n-1)}{2} \Gamma^2 \left( \frac{\partial u}{\partial z} \right)^2 \frac{\partial^2 u}{\partial z^2} \right) - \frac{\sigma B_0^2}{\rho} u, \quad (4)$$

$$\left( \frac{\partial v}{\partial t} + u \frac{\partial v}{\partial x} + v \frac{\partial v}{\partial y} + w \frac{\partial v}{\partial z} \right) = \nu \left( \left( 1 + \frac{1}{\beta} \right) \frac{\partial^2 v}{\partial z^2} + \frac{3(n-1)}{2} \Gamma^2 \left( \frac{\partial v}{\partial z} \right)^2 \frac{\partial^2 v}{\partial z^2} \right) - \frac{\sigma B_0^2}{\rho} v, \quad (5)$$

Where  $u, v$  and  $w$  are the velocity components along the  $x, y$  and  $z$  directions respectively.  $\nu$  is the kinematic viscosity coefficient,  $\beta$  is the Casson fluid parameter,  $\Gamma$  is the time constant,  $\rho$  is the density of the fluid and  $\sigma$  is the electric conductivity.

With the boundary conditions

$$\left. \begin{aligned} u = u_w(x) = \frac{ax}{(1-ct)}, v = v_w(x) = \frac{ax}{(1-ct)}, w = 0, \quad \text{at } z = 0, \\ u = v = 0, \quad \text{as } z \rightarrow \infty, \end{aligned} \right\} \quad (6)$$

Here  $u_w$  and  $v_w$  are the stretching velocities near the surface. To convert the nonlinear partial differential equations for velocities, we are now introducing the similarity transformations are given by:

$$\left. \begin{aligned} u = \frac{bx}{(1-ct)} f'(\eta), v = \frac{by}{(1-ct)} g'(\eta), w = -\frac{bv}{1-ct} (f(\eta) + g(\eta)) \\ \eta = \sqrt{\frac{b}{\nu_f(1-ct)}} z, \end{aligned} \right\} \quad (7)$$

Here in Equation (7)  $u, v$  and  $w$  are automatically satisfy the continuity equation, by using equation (7), the equations (3) to (5) are given by:

$$\left( 1 + \frac{1}{\beta} \right) f''' + (f + g) f'' - f'^2 - A(f' + \eta \frac{1}{2} f'') + \frac{3(n-1)}{2} We f'^2 f''' - M f' = 0, \quad (8)$$

$$\left( 1 + \frac{1}{\beta} \right) g''' + (f + g) g'' - g'^2 - A(g' + \eta \frac{1}{2} g'') + \frac{3(n-1)}{2} We g'^2 g''' - M g' = 0, \quad (9)$$

The transformed boundary conditions are:

$$\left. \begin{aligned} f = 0, g = 0, f' = \lambda, g' = \lambda, \quad \text{at } \eta = 0, \\ f' \rightarrow 0, g' \rightarrow 0, \quad \text{as } \eta \rightarrow \infty, \end{aligned} \right\} \quad (10)$$

here  $A$  is the unsteadiness parameter,  $We$  is the Weissenberg number,  $M$  is the magnetic field and  $\lambda$  is the stretching ratio parameter.

$$M = \frac{\sigma B_0^2}{\rho_f c}, We = \frac{\Gamma^2 x^2 b^3}{\nu(1-ct)^3}, \lambda = \frac{a}{b}, A = \frac{c}{b} \quad (11)$$

### Heat Transfer analysis:

The boundary layer thermal energy equation with nonlinear thermal radiation and non-uniform heat source/sink effect is given by

$$\frac{\partial T}{\partial t} + u \frac{\partial T}{\partial x} + v \frac{\partial T}{\partial y} + w \frac{\partial T}{\partial z} = \alpha \frac{\partial^2 T}{\partial z^2} + \frac{16\sigma^*}{3k\rho c_p} \frac{\partial T}{\partial z} \left( T^3 \frac{\partial T}{\partial z} \right) + q''' \quad (12)$$

With the boundary conditions are

$$T = T_w, \text{ at } z = 0, T \rightarrow T_\infty, \text{ as } z \rightarrow \infty, \quad (13)$$

The non-dimensional temperature is given by

$$T = T_\infty + (T_w - T_\infty)\theta, T = T_\infty(1 + (\theta_w - 1)\theta) \quad (14)$$

Where  $T$  is the fluid temperature,  $T_w, T_\infty$  are the near the fluid temperature and the far away from the fluid temperature,  $k$  is the thermal conductivity of the fluid,  $c_p$  is the specific heat capacitance at constant pressure,  $c_s$  is the concentration susceptibility and  $\sigma^*$  is the Stefan-Boltzmann constant.

The time dependent non-uniform heat source/sink  $q'''$  defined as

$$q''' = \frac{k_f u_w(x)}{x\nu} \left( A^*(T_w - T_\infty)f' + B^*(T - T_\infty) \right), \quad (15)$$

The above equation positive values of  $A^*, B^*$  corresponds to heat generation and negative values are corresponds to heat absorption.

By substituting the equation (14) into (12) and conditions (13) the equations are reduced to

$$\theta'' + \text{Pr}(f + g)\theta' - \frac{A}{2}\eta\theta' + A^*f' + B^*\theta + R\left( (1 + (\theta_w - 1)\theta)^3 \theta'' + 3(\theta_w - 1)\theta'^2 (1 + (\theta_w - 1)\theta)^2 \right) = 0, \quad (16)$$

With the transformed boundary conditions are

$$\theta(0) = 1, \theta(\infty) = 0, \quad (17)$$

Where  $\text{Pr}$  is the Prandtl number,  $A$  is the unsteadiness parameter,  $R$  is the thermal radiation parameter,  $\theta_w$  is the ratio of temperatures which are given by

$$\text{Pr} = \frac{k}{\mu C_p}, R = \frac{16\sigma^* T_\infty^3}{3kk^*}, \theta_w = \frac{T_\infty}{T_w}, \quad (18)$$

For physical quantities of interest the friction factor coefficients along  $x, y$  directions, local Nusselt numbers are given by

After using the boundary layer approximations wall shear stress  $\tau_w$  is given by

$$\tau_w = \frac{\partial u}{\partial x} + \frac{(n-1)\Gamma^2}{2} \left( \frac{\partial u}{\partial z} \right)^3, \quad (19)$$

The skin friction is defined by

$$C_{fx} \text{Re}^{1/2} = \frac{\tau_w}{\rho u_w(x)^2}, \text{Re}^{1/2} C_{fy} = \frac{\tau_w}{\rho u_w(y)^2}, \quad (20)$$

$$C_{fx} \text{Re}^{1/2} = \left[ \left( 1 + \frac{1}{\beta} \right) f''(0) + \frac{(n-1)We}{2} (f''(0))^3 \right], \text{Re}^{1/2} C_{fy} = \left[ \left( 1 + \frac{1}{\beta} \right) g''(0) + \frac{(n-1)We}{2} (g''(0))^3 \right], \quad (21)$$

$$\text{Re}^{-1/2} Nu_x = -\theta'(0). \quad (22)$$

Where  $Re = \frac{xu_w(x)}{\nu}$  is the Reynolds number.

### Results and Discussion

The set of nonlinear ordinary differential equations (8), (9) and (16) corresponding to the boundary conditions (10) and (17) are solved numerically using Runge-Kutta based shooting technique. Results display the influence of non-dimensional governing parameters on velocity and temperature profiles along with the friction factors and local Nusselt numbers. For numerical values we considered the non-dimensional parameter values as  $A=0.2, M=2, \eta=5, n=3, \beta=0.2, We=0.3, A^*=0.1, B^*=0.2, R=0.3, \theta_w=1.1, Pr=6.2$ . These values are kept as common in entire study except the variations in respective figures and tables. In graphical results red color profiles indicates the flow over a Carreau fluid stretching surface while green color profiles indicates the flow over a Casson fluid stretching surface.

The Figs. 1-3 presents the effect of stretching ratio parameter on velocity and temperature variations for both the Carreau and Casson fluid cases. The temperature field is suppressed and velocity field is improved with an increasing value of stretching ratio parameter. Basically, the stretching keeps more pressure on the sheet due to this the temperature field is reduced and velocity fields are encouraged. Figs. 4-6 depict the influence of Weissenberg number on velocity fields and temperature fields for both Carreau and Casson fluid cases. It is found that an increasing in the Weissenberg number enhances the thermal boundary layers and decreases the momentum boundary layer on the flow over a stretching surface for both the cases. Physically, Weissenberg number is directly proportional to the time constant and inversely proportional to the viscosity. The time constant to viscosity ratio is higher for larger values of Weissenberg number. Hence, higher Weissenberg number causes to enhance the thermal boundary thickness.

The dimensionless temperature distribution for different values of radiation parameter  $R$  is shown in Fig. 7 for both Carreau fluid Casson fluid cases. It reveals that the greater values of radiation parameter show an enhancement in the temperature boundary layer thickness. Generally, the greater values of radiation parameter produce more heat to working fluid that shows an enhancement in the temperature field. It is evident to mention here that we have noticed enhancement in the temperature profiles for both Carreau and Casson fluid stretching cases. The ratio of temperature on temperature profiles are shown in Fig. 8 for both Carreau and Casson fluid cases. It is clear from that an increasing value of temperature ratio parameter improves the temperature profiles. The effect of the magnetic field on velocity and temperature fields are displayed in Figs. 9-11 for both Carreau fluid and Casson fluid cases. We observed that the velocity, concentration fields are reduced and boots up the temperature field. This proves the general physical behavior of  $M$  that an improved values of  $M$  depreciates the velocity fields. Generally, the drag force increase and as a result depreciation occurs in the velocity field. The influence of an unsteadiness parameter on velocity, temperature and concentration fields is exhibit in Figs. 12-13 for both Carreau fluid and Casson fluid cases. We detect from the figure that the velocity fields are enhanced and reducing the temperature field with an increasing values of unsteadiness parameter. An increasing unsteadiness the less heat would be transferred to the sheet there may be due to this the temperature field is decreased.

Figs. 14 and 15 demonstrate the effect of non-uniform time dependent heat source/sink parameter on temperature distribution of the flow for both Carreau and Casson fluid cases. It is clear that an increasing value of space and temperature dependent heat source/sink parameters enhances the thermal boundary layer thickness of the flow over a stretching sheet for both Carreau fluid and Casson fluid cases. Generally, the non-uniform heat source/sink parameters acts as heat generators, which releases the heat energy to the flow and enhances the temperature profiles. Table 1 displays the Validation of the present results with the existed literature under some limited case. We found a better agreement of the present results with the existed literature. This proves the validity of the present results along with the accuracy of the numerical technique we used in this study. Tables 2 and 3 display the variations in the friction factors and local Nusselt numbers for Carreau fluid and Casson fluid cases for various values of non-dimensional governing parameters. It is noticed from the table that hike in the values of an unsteadiness parameter enhances the friction factor coefficients and heat transfer rate for both Carreau and Casson fluid cases. But we observed an interesting result that an increase in unsteadiness parameter enhances the friction factor for both Carreau and Casson fluid cases. We have seen exactly opposite results are observed in the presence of magnetic field parameter and Weissenberg number for both Carreau and Casson fluid cases. The rise in the values of non-uniform heat source/sink parameter does not influence the friction factor and it reduces the nusselt number for both Carreau and Casson fluid cases. We have observed same type of results with an increase in thermal radiation parameter.

Table.1 Validation of the Nusselt number with some limited case for different values of  $\beta \rightarrow \infty, We = \eta = R = A = A^* = B^* = \theta_w = 0, n = 1$ .

Pr = 0.7		Pr = 1		Pr = 10		
$\lambda \downarrow$	$-\theta'(0)$ Anilkumar and Roy[21]	$-\theta'(0)$ Present	$-\theta'(0)$ AnilKumar and Roy[21]	$-\theta'(0)$ Present	$-\theta'(0)$ AnilKumar and Roy[21]	$-\theta'(0)$ Present
0	0.4305	0.4305	0.557294	0.5572	1.4042	1.4042
1	0.6127	0.6004	0.721982	0.7219	1.5885	2.0911
10	1.0175	1.0172	1.170983	1.1709	2.3528	2.7734

Table.3 the physical parameter values of  $f''(0), g''(0)$  and  $-\theta'(0)$  for Casson and Carreau fluid cases different values

of  $M = 5, \beta = 0.2, We = 0, \eta = 5, R = 0.3, A = 0.2, \lambda = 0.2, A^* = 0.1, B^* = 0.1, \theta_w = 1.1, Pr = 6.2$ .

M	R	A	We	$\lambda$	$\theta_w$	A*	B*	Skin		Nus	
								Casson	Carreau	Casson	Carreau
1								-0.27540	-0.234429	0.805253	0.848403
2								-0.42189	-0.354917	0.709147	0.767788
3								-0.61227	-0.478409	0.630938	0.701860
	1							-0.91227	-0.478409	0.762170	0.630469
	2							-0.91227	-0.478409	0.564206	0.525606
	3							-0.91227	-0.478409	0.495495	0.472131
		1						-0.35005	-0.281248	0.790376	0.822788
		2						-0.21155	-0.198141	0.897563	0.879240
		3						-0.17077	-0.162777	0.951181	0.907927
			1					-5.92220	-0.865536	0.411890	0.580487
			3					-8.09415	-1.453479	0.353705	0.536758
			5					-10.6972	-2.553512	0.308190	0.499935
				0.2				-2.35482	-0.354917	0.698757	0.769758
				0.4				-9.61557	-1.409036	1.099698	1.226592
				0.6				-12.0837	-4.205586	1.407654	1.545336
					0.2			-1.25649	-0.328418	1.459806	1.742124
					0.4			-1.25649	-0.328418	1.315956	1.597801
					0.6			-1.25649	-0.328418	1.124242	1.303902
						1		-0.26848	-0.935648	0.648340	0.555206
						2		-0.26848	-0.935648	0.547861	0.504005
						3		-0.26848	-0.935648	0.447312	0.452794
							0.2	-1.36482	-0.372454	0.586801	0.748906
							0.3	-1.35642	-0.372454	0.481475	0.680504
							0.4	-1.35642	-0.372454	0.339267	0.603163

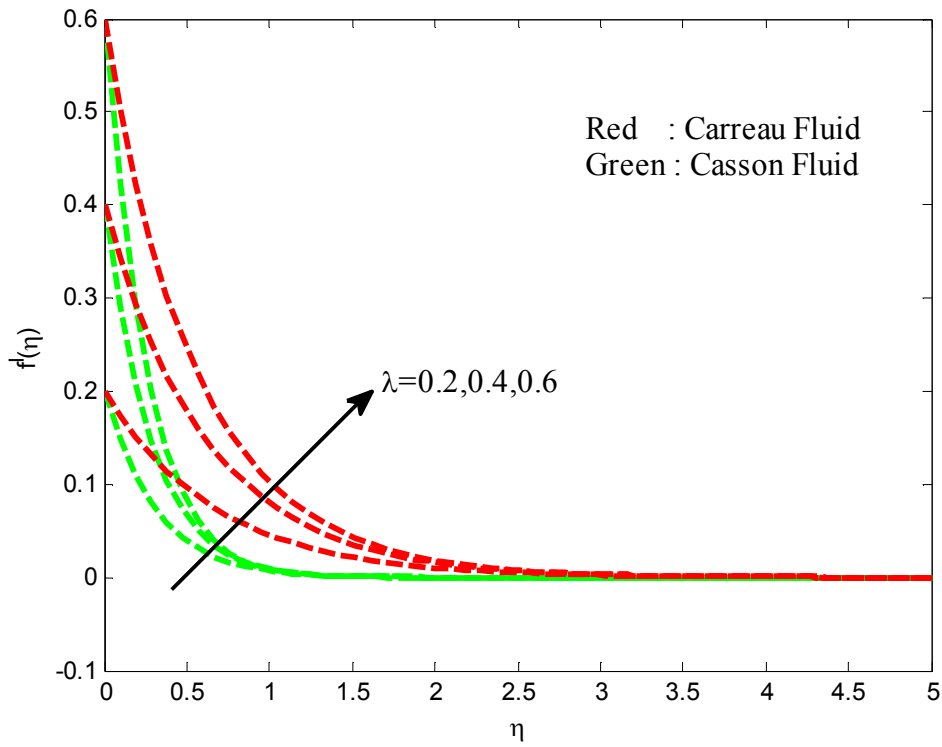


Fig.1 Velocity field for different values of stretching ratio parameter

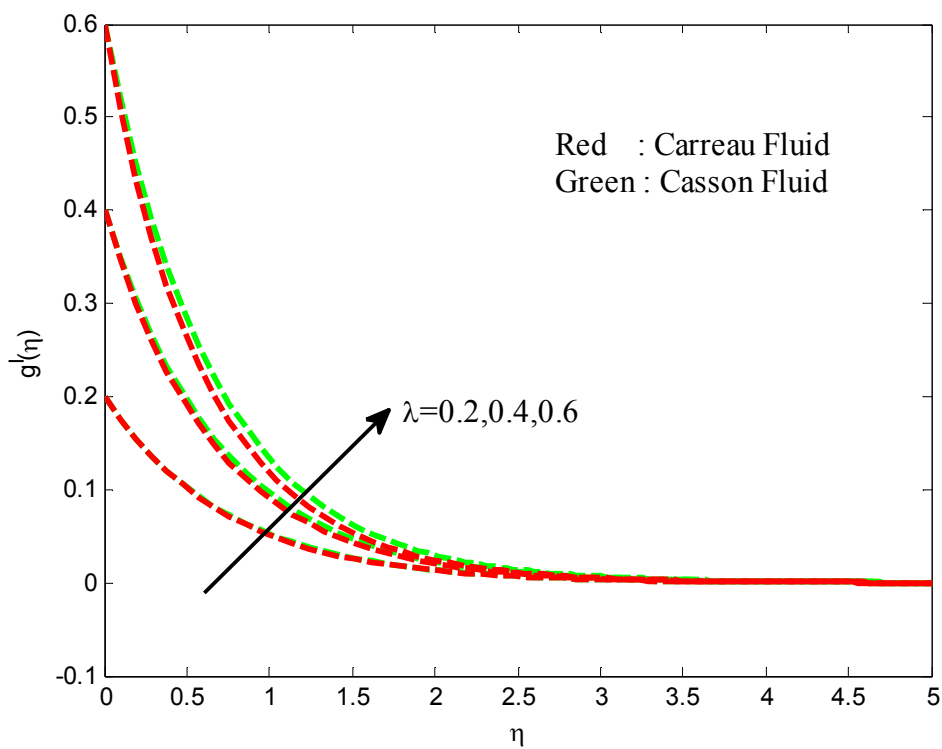


Fig.2 Velocity field for different values of stretching ratio parameter

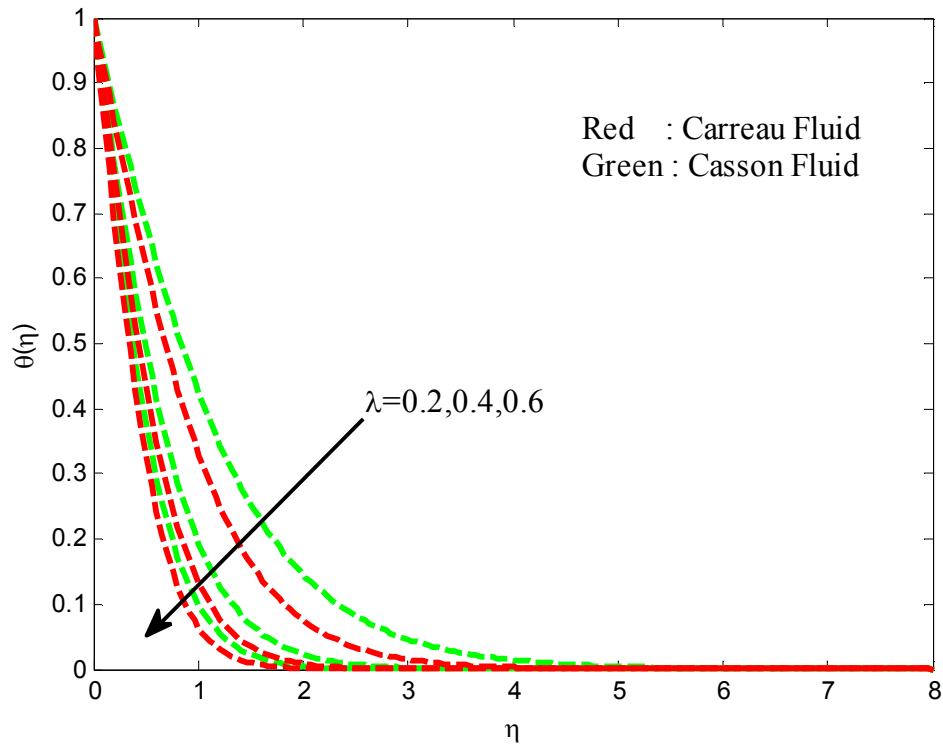


Fig.3 Temperature filed for different values of stretching ratio parameter

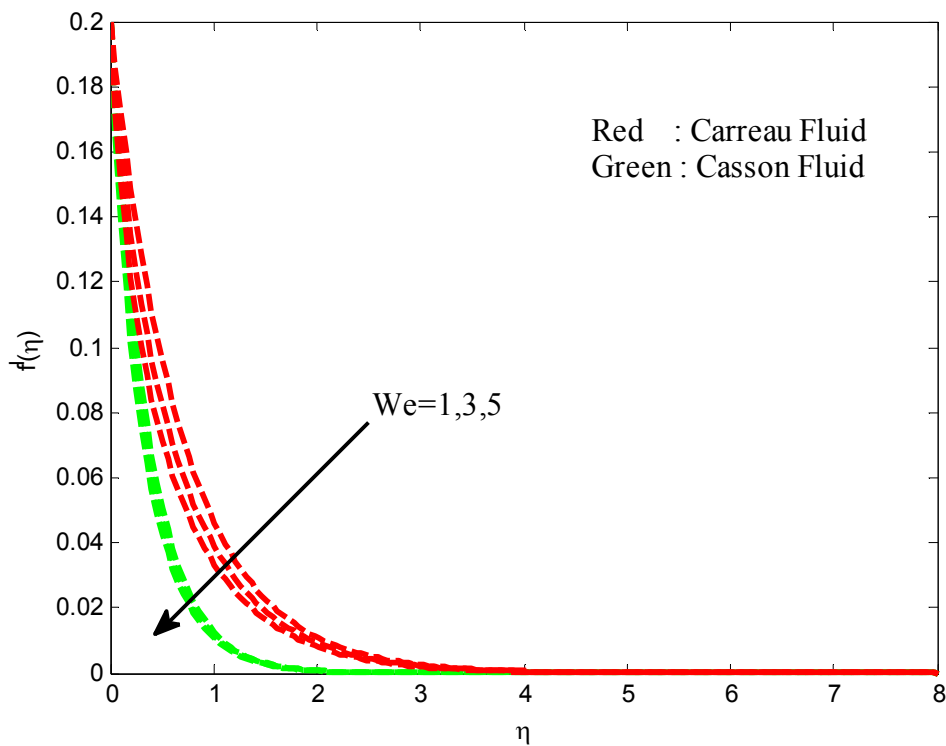


Fig.4 Velocity filed for different values of Weissenberg number

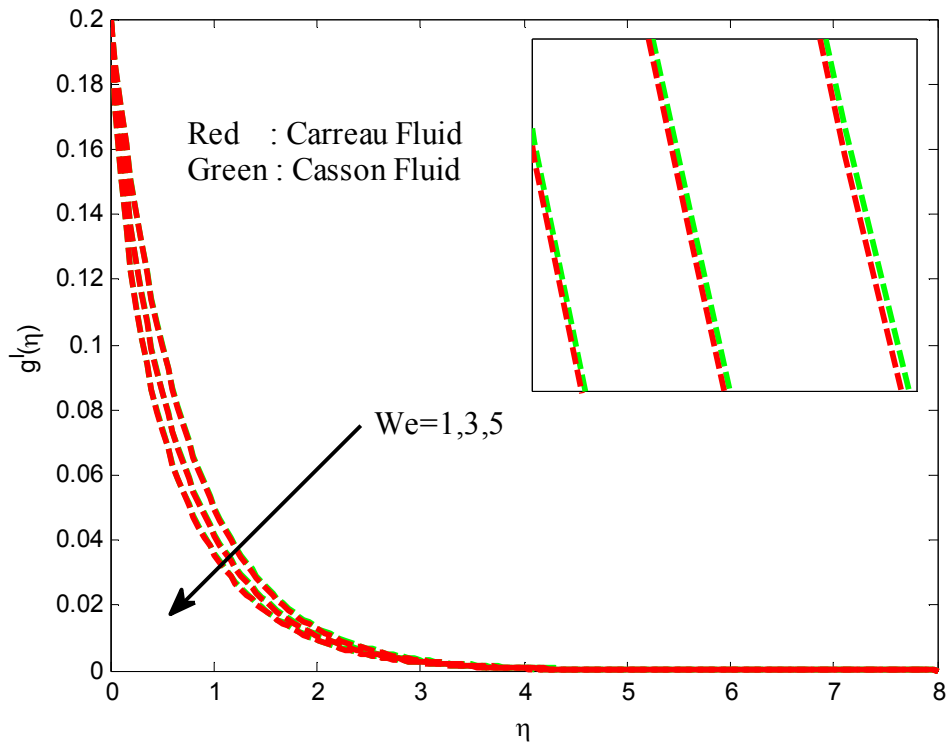


Fig.5 Velocity filed for different values of Weissenberg number

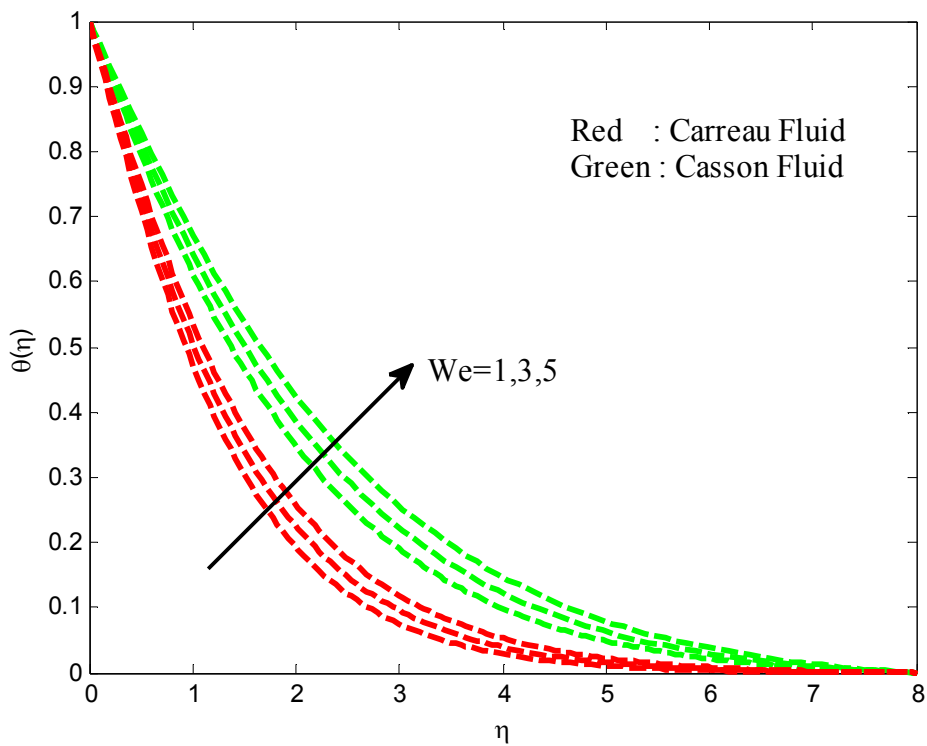


Fig.6 Temperature filed for different values of the Weissenberg number

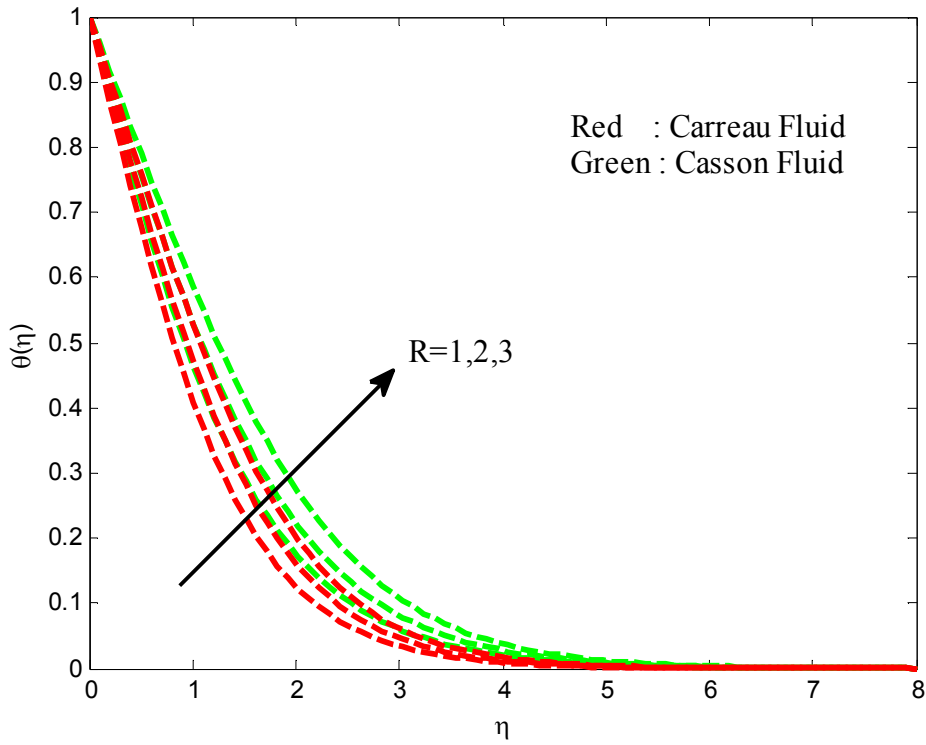


Fig.7 Temperature field for different values of radiation parameter

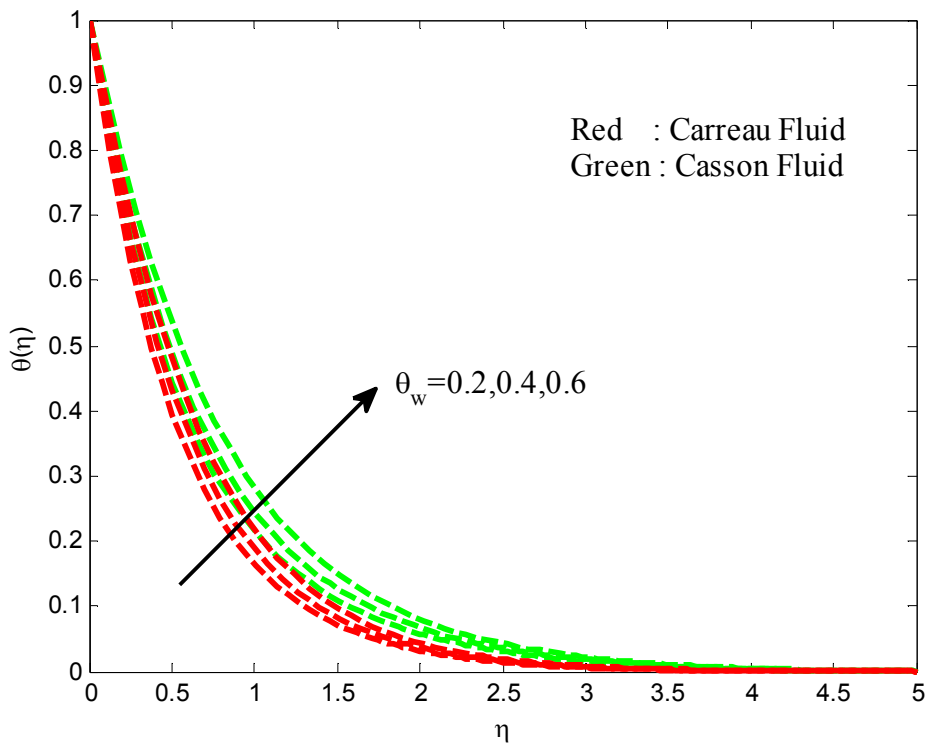


Fig.8 Temperature field for different values of ratio of temperature parameter

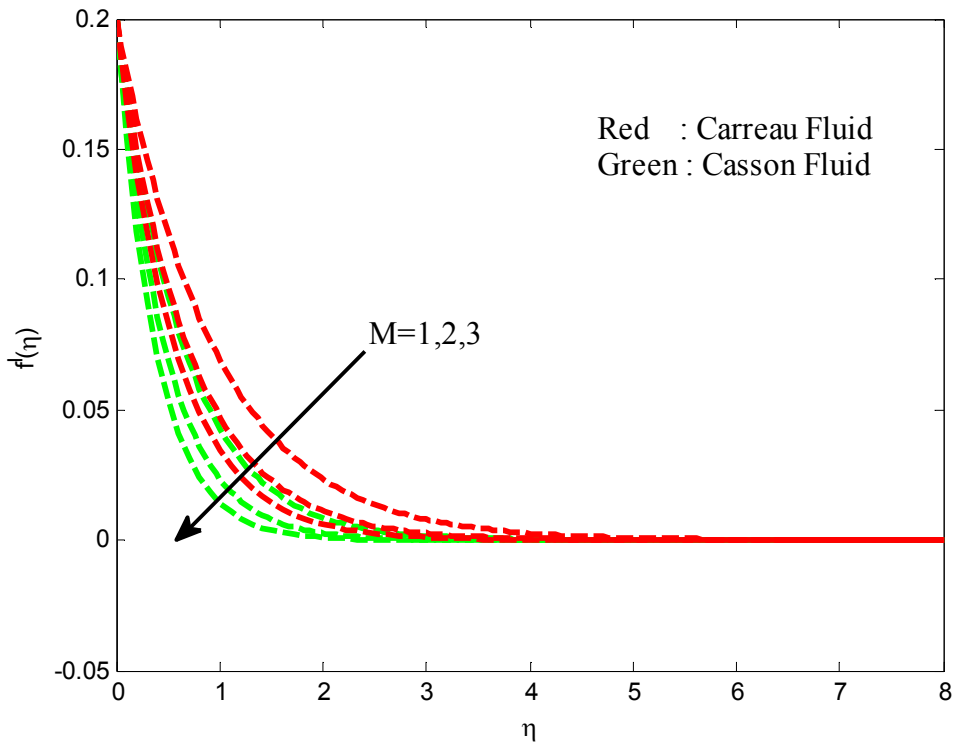


Fig.9 Velocity field for different values of magneticfield parameter

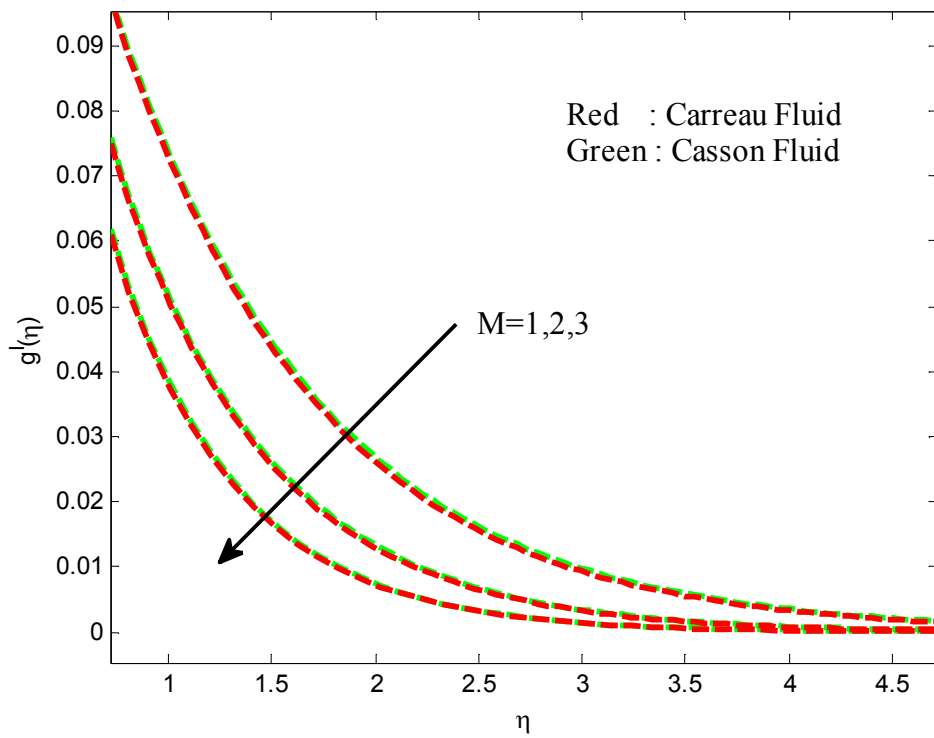


Fig.10 Velocity field for different values of Magneticfield parameter

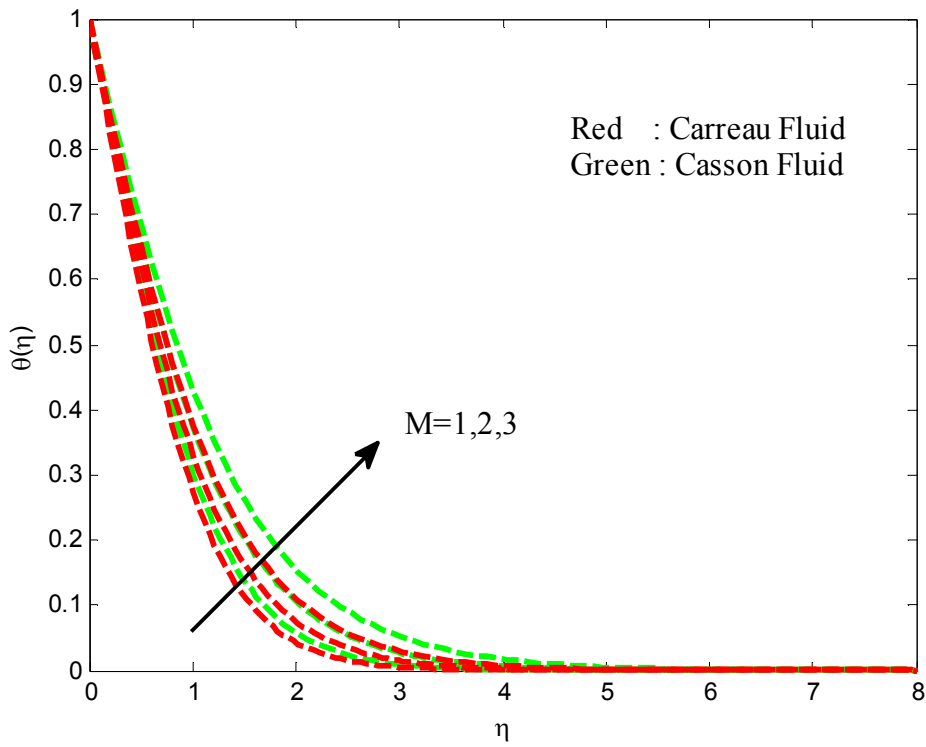


Fig.11 Temperature filed for different values of magneticfield parameter

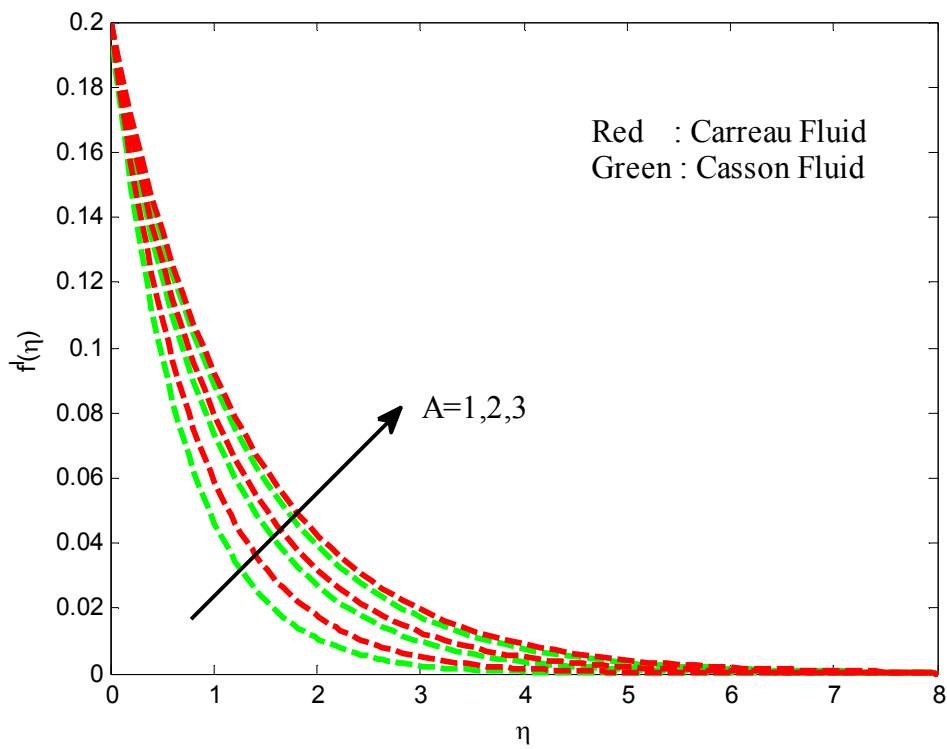


Fig.12 velocity filed for different values of an unsteadiness parameter

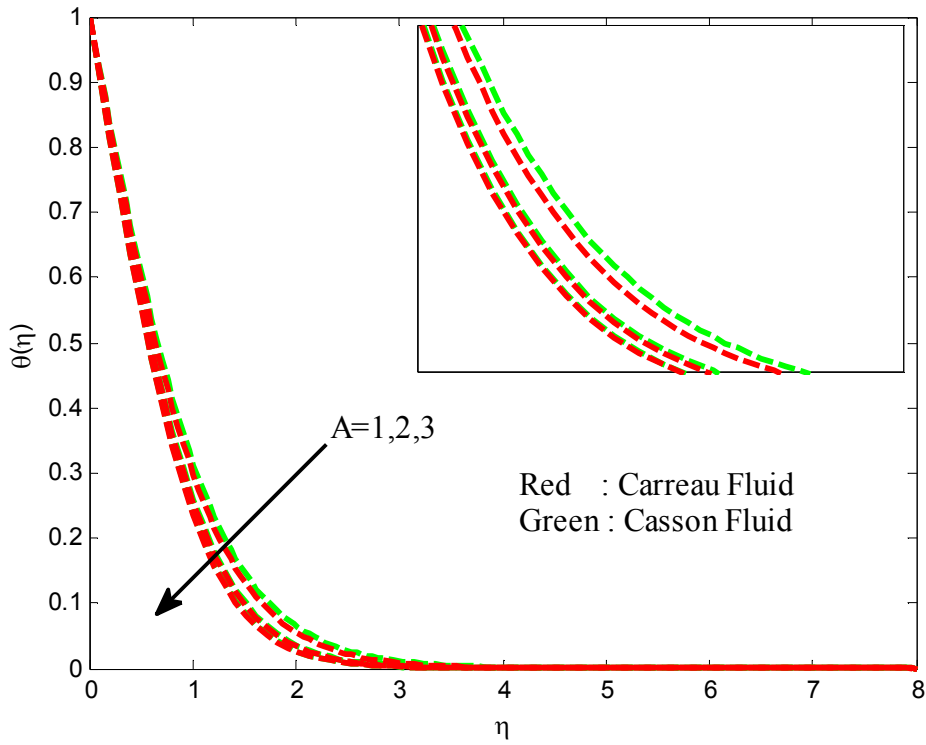


Fig.13 Temperature filed for different values of an unsteadiness parameter

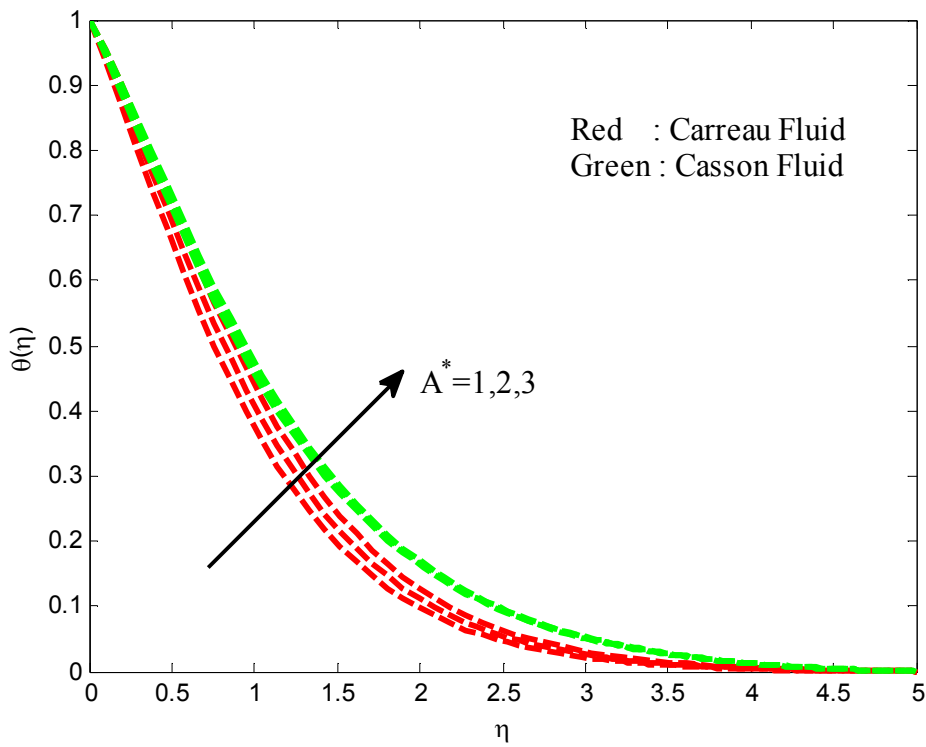


Fig.14 Temperature filed for different values of non-uniform heat source/sink parameter

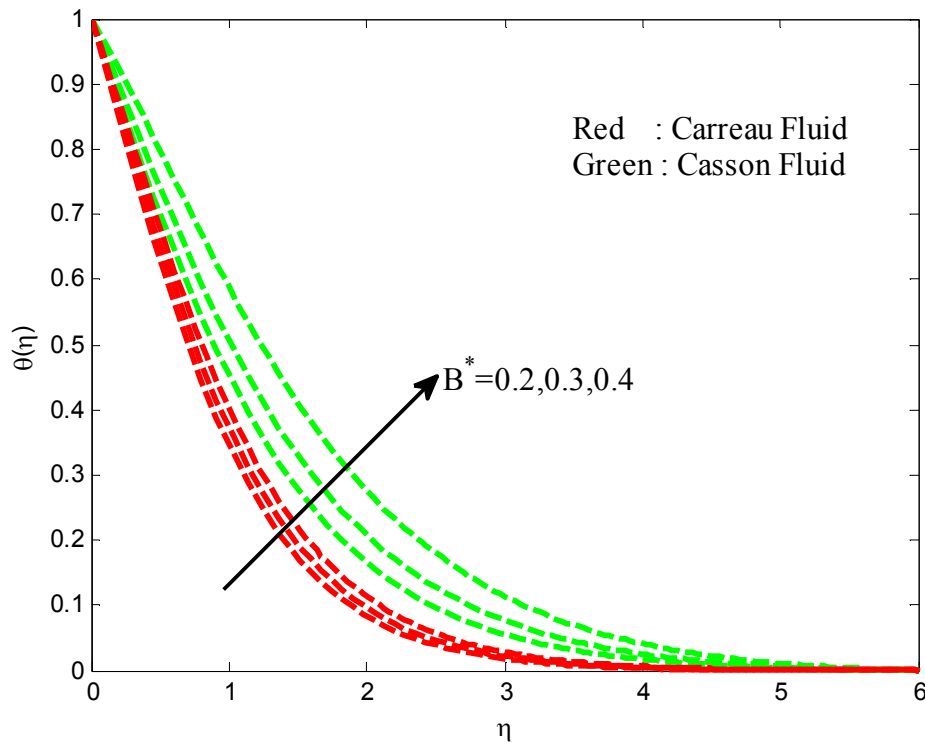


Fig.15 Temperature filed for different values of non-uniform heat source/sink parameter

#### Conclusions:

In this study, we proposed mathematical model for the effects of nonlinear thermal radiation on three-dimensional flow of Carreau and Casson fluid flow past a stretching surface with non-uniform heat source/sink. The transformed governing equations are solved numerically using Runge-Kutta based shooting technique. We obtained good accuracy of the present results by comparing with the exited literature. The influence of dimensionless parameters on velocity, temperature and concentration profiles along with the friction factors and local Nusselt numbers are discussed with the help of graphs and tables. We presented dual solutions for the flow over a Carreau and Casson fluid over a stretching sheet. The conclusions are as follows:

1. The heat transfer rate is more on Carreau fluid flow over stretching sheet when compared with Casson fluid over a stretching sheet.
2. Non-uniform heat source/sink and radiation parameters are help to reducing the nusselt number for both Carreau fluid Casson fluid cases.
3. The Weissenberg number and magneticfield parameters are improves the mass transfer rate.
4. An unsteadiness parameter increases the friction factor coefficients as well as heat transfer rate for the Casson and Carreau fluid cases.

#### References

- [1]. B.C Sakiadis, Boundary layer behavior on continuous solid surfaces, AICHE J., 7(1) (1961) 26-28.
- [2]. N. Bachok, A. Ishak, I. Pop, Boundary-layer flow of nanofluids over a moving surface in a flowing fluid, Int. J. Thermal Sci. 49(9) (2010) 1663-1668.
- [3]. L. Zheng, L. Wang, X. Zhang, Analytic solutions of unsteady boundary flow and heat transfer on a permeable stretching sheet with non-uniform heat source/sink, J. of Communications in Nonlinear Science and Numerical Simul. 16(2) (2011) 731-740.
- [4]. J. Harris, Rheology and Non-Newtonian flow, Longman, 1977.
- [5]. R. B. Bird, C. F. Curties, R. C. Armstrong, O. Hassager, Dynamics of polymeric liquids, Wiley, 1987.
- [6]. J. Zhu, Drag and Mass transfer for flow of a carreau fluid past a swarm of Newtonian drops, Int. J. Multiphase Flow 21(5) (1995) 935-940.
- [7]. G. C. Georgiou, The time-dependent, compressible poiseuille and extrudate-swell flows of a carreau fluid with slip at the wall, J. Non-Newtonian Fluid Mechanics, 109 (2003) 93-114.
- [8]. A. H. Abd El Naby, A. E. M. Ei Misery, M. F. AbdEl Kareem, Separation in the flow through peristaltic motion of a carreau fluid in uniform tube, Physica A 343 (2004) 1-14.

- [9]. C.S. K. Raju, N. Sandeep, Falkner Skan flow of a magnetic Carreau fluid past a wedge in the presence of cross diffusion, *European Physical Journal Plus*, 131 (2016) 267.
- [10]. Kh. S. Mekheimer, Effect of the induced magnetic field on peristaltic flow of a couple stress fluid, *Physics Letters A* 372 (2008) 4271-4278.
- [11]. T. Hayat, N. Saleem, N. Ali, Effect of induced magnetic field on peristaltic transport of a Carreau fluid, *Commun Nonlinear Sci. Numeric. Simul.* 15 (2010) 2407-2423.
- [12]. C. S. K. Raju, N. Sandeep, C. Sulochana, V. Sugunamma, Effects of aligned magnetic field and radiation on the flow of ferrofluids over a flat plate with non-uniform heat source/sink, 8(2) (2015) 151-158.
- [13]. N. S. Akbar, S. Nadeem, Z. H. Khan, Numerical simulation of peristaltic flow of a Carreau nanofluid in an asymmetric channel, *Alexandria Engineering J.* 53 (2014) 191-197.
- [14]. C. S. K. Raju, M. Jayachandrababu, N. Sandeep, Chemically reacting radiative MHD Jefferey nanofluid flow over a cone in porous medium, *Int. J. Eng. Res. In Africa* 19 (2016) 75-90.
- [15]. M. N. Mahantesh, M. Subhas Abel, J. Tawade, Heat transfer in a Walter's liquid B fluid over an impermeable stretching sheet with non-uniform heat source/sink and elastic deformation, *J. Communications in Nonlinear Science and Numerical Simul.* 15(7) (2010) 1791-1802.
- [16]. A. Khalid, I. Khan, S. Shafie, Exact solutions for unsteady free convection flow of casson fluid over an oscillating vertical plate with constant wall temperature, *Abstract and Applied Analysis Article Id: 946350* (2015) <http://dx.doi.org/10.1155/2015/946350>.
- [17]. M. Jayachandrababu, N. Sandeep, C. S. K. Raju, Heat and mass transfer in MHD Eyring-Powell nanofluid flow due to cone in porous medium, *Int. J. Eng. Res. In Africa* 19 (2015) 57-74.
- [18]. T. Hayat, A. Asad, M. Mustafa, A. Alsaedi, Boundary layer flow of Carreau fluid over a convectively heated stretching sheet, *Applied Mathematics and Computation* 246 (2014) 12-22.
- [19]. C. S. K. Raju, N. Sandeep, V. Sugunamma, M. Jayachandrababu, J. V. Ramanareddy, Heat and mass transfer in magnetohydrodynamic Casson fluid over an exponentially permeable stretching surface, *Engineering Science and Technology, An International* (2015) DOI:10.1016/j.jestch.2015.05.010.
- [20]. N. S. Akbar, S. Nadeem, R. UI Haq, S. Ye, MHD stagnation point flow of Carreau fluid toward a permeable shrinking sheet: Dual solutions, *Ain Shams Eng. J.* 5 (2014) 1233-1239.
- [21]. D. Anilkumar, S. Roy, Unsteady mixed convection flow on a rotating cone in rotating fluid, *Appl. Math. Computation* 155 (1963) 545-561.
- [22]. S. Nadeem, R. UI Haq, N. S. Akbar, Z. H. Khan, MHD three-dimensional casson fluid flow past a porous linearly stretching sheet, *Alexandria Eng. J.* 52 (2013) 577-582.
- [23]. C.S. K. Raju, N. Sandeep, Unsteady Casson nanofluid flow over a rotating cone in a rotating frame filled with ferrous nanoparticles: A Numerical study, *Journal of Magnetism & Magnetic Materials*, DOI: <http://dx.doi.org/10.1016/j.jmmm.2016.08.013>.
- [24]. S.M. Ibrahim, G. Lorenzini, P. Vijayakumar, C.S. K. Raju, Influence of chemical reaction and heat source on dissipative MHD mixed convection flow of a Casson nanofluid over a nonlinear permeable stretching sheet, *Int. J. Heat and Mass Transfer*, 11 (2017) 346-355.
- [25]. C. S. K. Raju, K. R. Sekhar, S. M. Ibrahim, G. Lorenzini, G. Viswanathareddy, E. Lorentzini, Variable viscosity on unsteady dissipative Carreau fluid over a truncated cone filled with titanium alloy nanoparticles, *Continuum Mechanics and Thermodynamics*, DOI 10.1007/s00161-016-0552-8.
- [26]. C.S. K. Raju, M.M. Hoque, T. Sivasankar, Radiative flow of Casson fluid over a moving wedge filled with gyrotactic microorganisms, *Advanced Powder Technology* 28(2) (2016) 575-583.
- [27]. C.S. K. Raju, P. Priyadarshini, S. M. Ibrahim, Multiple slip and cross-diffusion on MHD Carreau-Casson fluid over a slendering sheet with non-uniform heat source/sink, *Int. J. Appl. Compt. Math.*, Doi: 10.1007/s40819-017-0351-3.
- [28]. A.G. Madaki, R. Roslan, M.S. Rusiman, C. S. K. Raju, Analytical and numerical solutions of squeezing unsteady Cu and TiO<sub>2</sub>-nanofluid flow in the presence of thermal radiation and heat generation/absorption, in online, *Alexandria Engineering Journal*, <https://doi.org/10.1016/j.aej.2017.02.011>.
- [29]. Rashidi, M. M., Raju, C. S.K, Sandeep, N., & Saleem, S. (2016). A Numerical Comparative Study on 3D Nanofluid Flows. *Journal of Computational and Theoretical Nanoscience*, 13(8), 4835-4842.
- [30]. C. S. K. Raju, M.M. Hoque, N.N. Anika, S. U. Mamatha, S. Pooja, Natural convective heat transfer analysis of MHD unsteady Carreau nanofluid over a cone packed with alloy nanoparticles, *Powder Technology*, (2016) <https://doi.org/10.1016/j.powtec.2017.05.003>.